

ESTIMATE OF ACID DEPOSITION THROUGH FOG USING NUMERICAL MODELS IN THE KINKI REGION OF JAPAN

Hikari Shimadera^{1,2}, Akira Kondo¹, Akikazu Kaga¹, Kundan L. Shrestha^{1,2}, and Yoshio Inoue¹

¹Graduate School of Engineering, Osaka University, Japan

²Research Fellow of the Japan Society for the Promotion of Science (JSPS)

Abstract: Fog water deposition in forest areas can lead to the considerable amount of acid deposition. This study developed a two-dimensional fog water deposition model (FDM), and presented general features of FDM. A comparison of FDM with field measurement data showed that FDM often over- and underestimated the turbulent fog water fluxes, but captured the total amount. In order to estimate fog water deposition and corresponding acid deposition in the Kinki Region of Japan, FDM was utilized with results of meteorology and air quality predictions by the 5th generation PSU/NCAR Mesoscale Model (MM5) and the U.S. EPA's Models-3 Community Multiscale Air Quality modeling system (CMAQ) in March 2005. In mountainous areas, the amounts of fog water deposition ranged from 0 to 78.4 mm (mean = 9.1 mm), while rainfall ranged from 97.2 to 785.9 mm (mean = 270.8 mm). Consequently, ratios of fog water deposition to rainfall reached up to 22.5 %, ratios of sulfur depositions through fog to those through rain reached up to 52.5 %, and ratios of nitrogen depositions through fog to those through rain reached up to 96.9 %. The results indicated that fog water deposition contributed significantly to acid deposition in some mountainous areas in the Kinki Region.

Key words: Fog deposition model; Forest; MM5/CMAQ; sulfur and nitrogen depositions

INTRODUCTION

Fog can affect forest ecosystems in mountainous and coastal areas, in which fog occurs more frequently than in other areas. Fog water deposition through the interception of fog droplets by vegetation can be an important part of the hydrologic budget of forests (Vong et al., 1991; Dawson, 1998). Ionic concentrations in fog water are much higher than those in rain water (Neal et al., 2003; Aikawa et al., 2006). Consequently, fog can contribute significantly to the deposition of ionic compounds in mountainous forest areas. The effects of fog may be more pronounced in Japan than in other countries because approximately two-thirds of the land area is covered by forests, most of which are located in mountainous regions.

The amounts of fog water deposition have been measured using a variety of approaches, such as the through fall measurement (Kobayashi et al., 2001) and the eddy covariance method (Klemm et al., 2005). Numerical models also have been utilized to estimate fog water deposition. A one-dimensional model developed by Lovett (1984) has been widely used to predict turbulent deposition of fog in various mountain forests (Miller et al., 1993; Baumgardner et al., 2003). Katata et al. (2008) modified a one-dimensional land surface model called SOLVEG to better predict fog water deposition, and showed that the modified SOLVEG agreed better with the measurement data by Klemm et al. (2005) than the model developed by Lovett (1984).

The present study developed a two-dimensional fog water deposition model (FDM), and compared FDM with the field measurement. Moreover, FDM was utilized to estimate fog water deposition and corresponding acid deposition in the Kinki Region of Japan with the results of meteorology and air quality predictions by the 5th generation Penn State University/National Center for Atmospheric Research Mesoscale Model (MM5) (Grell et al. 1994) version 3.7 and the U.S. Environmental Protection Agency's Models-3 Community Multiscale Air Quality modeling system (CMAQ) (Byun and Ching, 1999) version 4.7.

FOG DEPOSITION MODEL

Model structure

Equations to simulate turbulent airflow in and above a forest canopy are based on equations of mean motion and turbulence energy used by Yamada (1982). The horizontal wind direction is assumed to be constant in FDM. An equation of mean motion is

$$\frac{\partial u}{\partial t} = \frac{\partial}{\partial t} \left(K_M \frac{\partial u}{\partial z} \right) - C_d a_s(z) u |u|, \quad (1)$$

where u is the horizontal wind component (m s^{-1}), K_M is the eddy diffusivity of momentum ($\text{m}^2 \text{s}^{-1}$), $C_d (= 0.2)$ is the drag coefficient for a forest canopy and $a_s(z)$ is the one-sided surface area density ($\text{m}^2 \text{m}^{-3}$), which is the sum of the leaf area density ($a_l(z)$) and the non-leaf area density. The vertical distribution of $a_s(z)$ within a canopy is obtained from a function proposed by Kondo and Arakashi (1976) as

$$a_s(z) = \frac{SAI}{h_{fc}} \hat{a}(Z) \quad \text{for} \quad 0 \leq Z \leq 1, \quad (2)$$

$$Z = z/h_{fc}, \quad (3)$$

$$\hat{a}(Z) = a_m \frac{1-Z}{1-Z_m} \exp \left[\frac{1}{2} (Z_m - \lambda)^2 - \frac{1}{2} (Z - \lambda)^2 \right], \quad (4)$$

$$Z_m \begin{cases} = \frac{\lambda + 1 - \sqrt{(\lambda - 1)^2 + 4}}{2} & \text{for } \lambda > 1, \\ = 0 & \text{for } \lambda \leq 1, \end{cases} \quad (5)$$

where SAI is the one-sided canopy surface area index ($\text{m}^2 \text{m}^{-2}$), which is the sum of the leaf area index (LAI) and the non-leaf area index ($NLAI$), and h_{fc} is the forest canopy height, λ is a parameter, Z_m is the height at which $\hat{a}(Z)$ takes a maximum value, and a_m is a constant determined to satisfy

$$\int_0^1 \hat{a}(Z) dZ = 1. \quad (6)$$

An advection-diffusion equation of the liquid water content of fog (LWC) (kg m^{-3}) is

$$\frac{\partial LWC}{\partial t} = -u \frac{\partial LWC}{\partial x} - w \frac{\partial LWC}{\partial z} + \frac{\partial}{\partial z} \left(K_M \frac{\partial LWC}{\partial z} \right) - Dep. \quad (7)$$

The deposition term Dep is given by

$$Dep = f_L a_L(z) \varepsilon_{IM} |u| LWC, \quad (8)$$

where f_L is the portion of the effective leaf area for deposition of fog droplets and ε_{IM} is the impaction efficiency of fog droplet. According to Nagai (2002) and Katata et al. (2008), f_L and ε_{IM} can be expressed by

$$f_L = \frac{1 - \exp(-0.4 a_L(z) \Delta z)}{a_L(z) \Delta z}, \quad (9)$$

$$\varepsilon_{IM} = \left(\frac{\gamma St}{\gamma St + \alpha} \right)^\beta, \quad (10)$$

$$St = \frac{\rho_w d_p^2 |u|}{9 \mu_A d_L}, \quad (11)$$

where α , β and γ ($= 5.0, 1.05$ and 1 for needle leaf, and $0.5, 1.90$ and 5 for broad leaf, respectively) are fitting parameters, St is the Stokes number, ρ_w is the density of water (kg m^{-3}), d_p ($= 17.03 LWC \times 10^{-3} + 9.72 \times 10^{-6}$) is the mean diameter of fog droplet (m), μ_A is the viscosity coefficient of air ($\text{kg m}^{-1} \text{s}^{-1}$), d_L ($= 0.001$ m for needle leaf and 0.030 m for broad leaf) is the characteristic leaf length (m).

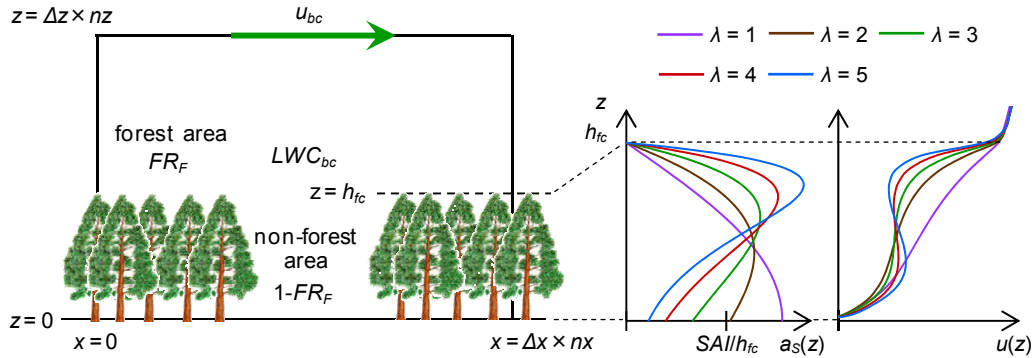


Figure 1. Schematic diagram of FDM.

Figure 1 shows the schematic diagram of FDM, where u_{bc} is u at the upper boundary, LWC_{bc} is LWC above the forest canopy, FR_F is the fraction of the area covered with forests, nx and nz are the number of the horizontal and the vertical grids, respectively. Forests are allocated to the computational area from its horizontal edges according to FR_F . The vertical distribution patterns of $a_s(z)$ vary with the values of λ . In this study, FDM predicted steady state u and LWC for each simulation case.

General features of the model

To show general features of FDM, calculations were conducted with the following conditions: the atmosphere was neutral, $u_{bc} = 0.5 \sim 10 \text{ m s}^{-1}$, $LWC_{bc} = 0.0003 \text{ kg m}^{-3}$, $h_{fc} = 18 \text{ m}$, $LAI = 0.1 \sim 10$, $NLAI = 0.5$, $FR_F = 0.24 \sim 0.96$, $\lambda = 3$, forest areas consisted of 100 % of needle-leaved trees, $\Delta x = 40 \text{ m}$, $nx = 50$, $\Delta z = 1.5 \text{ m}$, $nz = 30$. Figure 2 shows mean values of the fog water deposition velocity ($V_{Dep} = \text{fog water deposition flux}/LWC_{bc}$) in the computational area. Since ε_{IM} increases with increasing u , V_{Dep} increases with increasing u_{bc} . When forest areas are thin, V_{Dep} considerably increases with an increase in LAI . As a forest becomes denser, drag force induced by the vegetation surface becomes larger, resulting in smaller u within a canopy. Therefore, when forest areas are dense, V_{Dep} does not very increase or can decrease with an increase in LAI . The values of mean V_{Dep} in the case of $FR_F = 0.96$ are consistently (3.4 and 2.9 ($< 4 = 0.96/0.24$) times when $u_{bc} = 1$ and 10 m s^{-1} , respectively) larger than those in the case of $FR_F = 0.24$. Figure 3 shows horizontal distributions of V_{Dep} in the cases of $u_{bc} = 1$

m s^{-1} , $LAI = 3$ and $u_{bc} = 10 \text{ m s}^{-1}$, $LAI = 3$. The value of V_{Dep} at the windward edge of forest is the largest in every cases of FR_F , and increases with increasing width of the gap between forest areas.

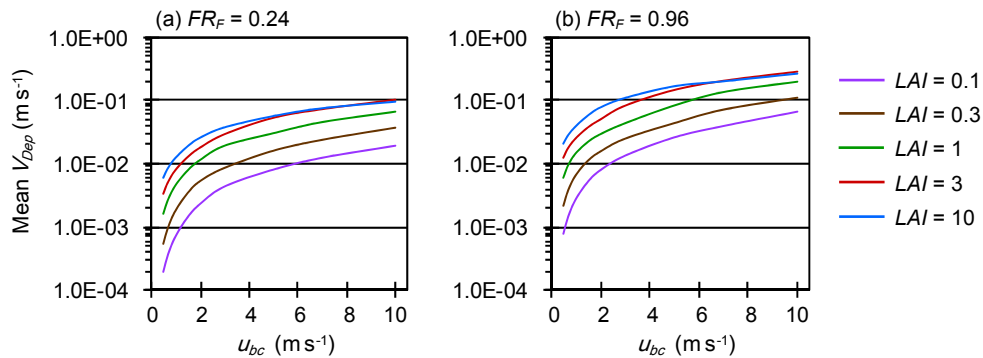


Figure 2. Mean V_{Dep} in the computational area plotted against u_{bc} in the cases of (a) $FR_F = 0.24$ and (b) $FR_F = 0.96$.

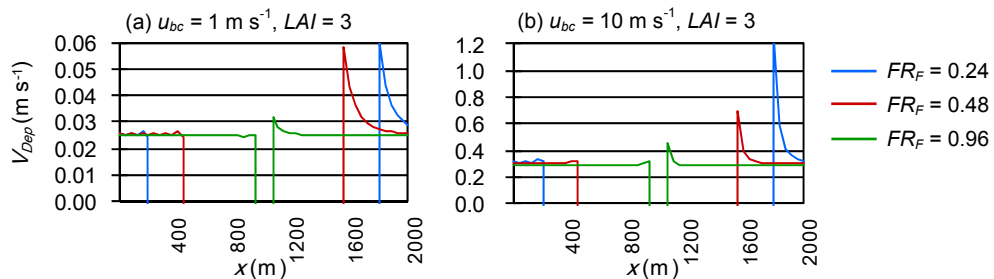


Figure 3. Horizontal distributions of V_{Dep} in the cases of (a) $u_{bc} = 1 \text{ m s}^{-1}$, $LAI = 3$ and (b) $u_{bc} = 10 \text{ m s}^{-1}$, $LAI = 3$.

Comparison with field measurement

Burkard et al. (2003) measured the turbulent fog water flux with the eddy covariance method at 45 m on a tower (15 m above the forest canopy) at a site ($47^{\circ}28'49''\text{N}$, $8^{\circ}21'05''\text{E}$, 690 m above sea level) on the Lägeren mountain, approximately 15 km northwest of Zurich, Switzerland. The vegetation cover around the site is mixed forest dominated by beech and Norway spruce. Fog water flux estimated by FDM was compared with the measurement for from September 2001 to March 2002. Calculations were conducted with the 30-minute measurement data and the following conditions: $h_{fc} = 30 \text{ m}$, LAI was derived from the monthly datasets of the MODIS LAI product, $NLAI = 0.5$, $FR_F = 1$, $\lambda = 3$, forest areas consisted of 50 % of needle-leaved trees and 50 % of broad-leaved trees, $\Delta x = 40 \text{ m}$, $n_x = 50$, $\Delta z = 1.5 \text{ m}$, $n_z = 30$. Figure 4 shows comparisons of the results of FDM with the field measurement data for accumulated turbulent fog water flux and V_{Dep} . While the total turbulent fog water flux in FDM (7.3 mm) agreed with that in the measurement (7.4 mm), large discrepancies often occurred between FDM and the measurement. As V_{Dep} in FDM strongly depend on u , FDM underestimated the magnitude of the fog water flux when V_{Dep} in the measurement was large despite low u_{bc} , and overestimated when V_{Dep} in the measurement was small despite high u_{bc} .

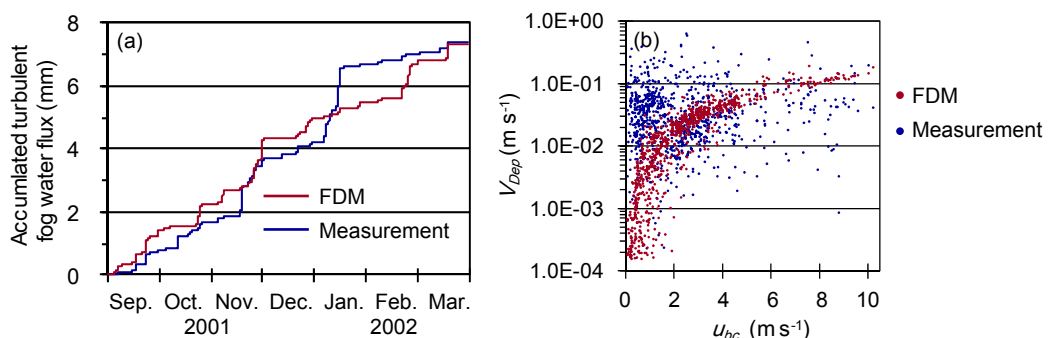


Figure 4. Comparisons of FDM with the field measurement for (a) accumulated turbulent fog water flux and (b) V_{Dep} plotted against u_{bc} from September 2001 to March 2002

FOG DEPOSITION IN KINKI REGION

Meteorology and air quality predictions

Input data for FDM were derived from the MM5/CMAQ modeling system to estimate fog water deposition and corresponding acid deposition in the Kinki Region of Japan. Shimadera et al. (2009) applied the MM5/CMAQ modeling system to meteorology and air quality predictions in March 2005. Figure 5 shows modeling domains for the meteorology and air quality predictions. The horizontal domains consist of 4 domains from domain 1 (D1) covering a wide area of East Asia to domain 4 (D4) covering most of the Kinki Region. The horizontal resolutions and the number of grid cells in the domains are 54, 18, 6 and 2 km, and 105×81 , 72×72 , 99×99 and 126×126 for D1, domain 2 (D2), domain 3 (D3) and D4,

respectively. The vertical layers consist of 24 sigma-pressure coordinated layers from the surface to 100 hPa with approximately 15, 50 and 110 m as the middle height of the first, second and third layer, respectively. The MM5/CMAQ modeling system well reproduced the meteorological fields and the long-range atmospheric transport from the Asian Continent to Japan in March 2005.

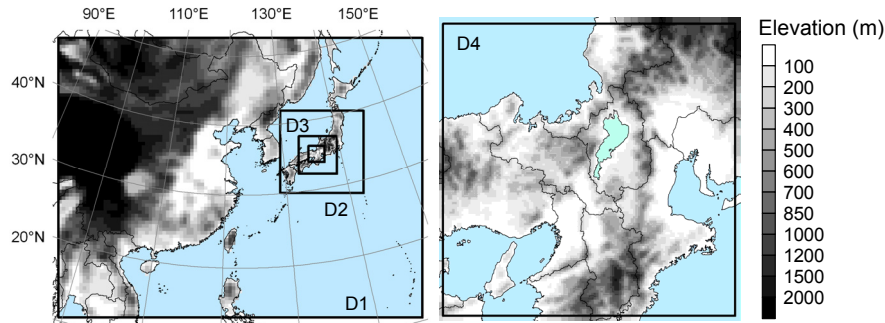


Figure 5. Modeling domains for the meteorology and air quality predictions.

Forest data

Parameters on forest, such as FR_F and LAI , are important in FDM as shown in figure 2. For an application of FDM to D4, FR_F was obtained from the 100-m land use dataset of the Digital National Land Information prepared by the Ministry of Land, Infrastructure, Transport and Tourism in Japan. LAI was derived from the monthly 1-km dataset of the MODIS LAI product for March 2005. Forest classes, including deciduous needle-leaved forest (DNF), evergreen needle-leaved forest (ENF), deciduous broad-leaved forest (DBF) and evergreen broad-leaved forest (EBF) were determined by using the 1-km vegetation dataset of the 5th National Survey on the Natural Environment conducted by the Ministry of the Environment in Japan. Figure 6 shows spatial distributions of FR_F , LAI and dominant forest class at each 2-km grid in D4. Forest areas account for 64.8 % of the land areas and 94.6 % of the mountainous areas (means areas with elevations > 500 m above sea level hereafter). DNF, ENF, DBF and EBF account for 0.3, 67.0, 28.5 and 4.2 % of the forest area, respectively. Because March is before or at the beginning of the vegetation growing season in D4, most of the forest areas tend to be thin and their LAI hardly reach 3. The north-eastern areas covered with DBF show the lowest LAI and the southern areas covered with ENF or EBF show relatively higher LAI .

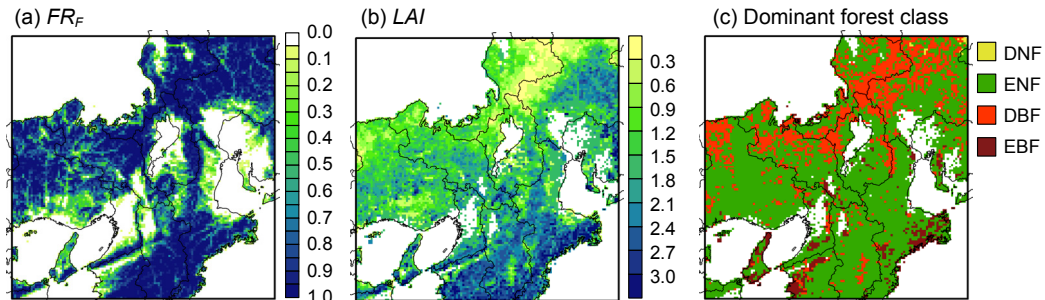


Figure 6. Spatial distributions of (a) FR_F , (b) LAI and (c) dominant forest class in D4.

Fog water deposition

The fog water deposition in D4 was estimated using FDM with the hourly MM5 results, the forest data described above, and the following conditions: $h_{fc} = 18$ m, $NLAI = 0.5$, $\lambda = 3$, $\Delta x = 40$ m, $n_x = 50$, $\Delta z = 1.5$ m, $n_z = 30$. Figure 7 shows spatial distributions of model-predicted frequency of fog occurrence, fog water deposition and rainfall in D4 in March 2005. The fog frequency, fog water deposition and rainfall generally increased with increasing elevation. The fog frequency and rainfall were the highest in the north-eastern area dominantly covered with DBF, but the fog water deposition was not due to the thin vegetation cover. This trend may change in the vegetation growing season. In the mountainous areas, the amounts of fog water deposition ranged from 0 to 78.4 mm (mean = 9.1 mm), while rainfall ranged from 97.2 to 785.9 mm (mean = 270.8 mm). Consequently, ratios of fog water deposition to rainfall ranged from 0 to 22.5 % (mean = 3.3 %).

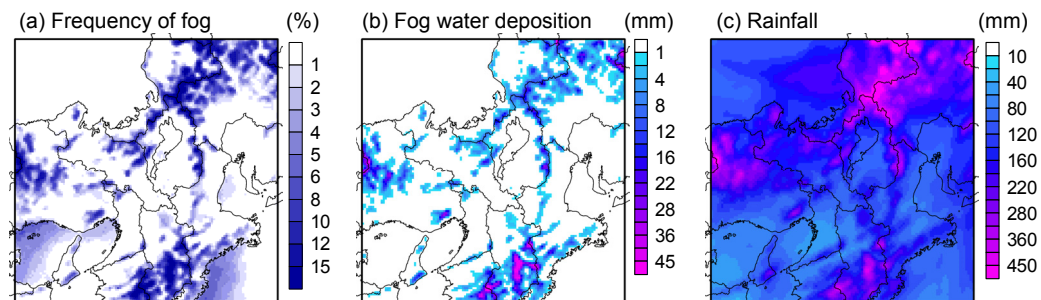


Figure 7. Spatial distributions of model-predicted (a) frequency of fog, (b) fog water deposition and (c) rainfall in D4 in March 2005.

Acid deposition

Sulfur (S) and reactive nitrogen ($\text{NO}_Y = \text{NO} + \text{NO}_2 + \text{NO}_3 + \text{N}_2\text{O}_5 + \text{HNO}_3 + \text{HONO} + \text{aerosol nitrate}$ in the present study) depositions through fog were estimated with the results of FDM and CMAQ. Figure 8 shows spatial distributions of model-predicted S and NO_Y depositions through fog, and S and NO_Y depositions through rain in D4 in March 2005. In the mountainous areas, ratios of S depositions through fog to those through rain ranged from 0 to 52.5 % (mean = 6.7 %), and ratios of NO_Y depositions through fog to those through rain ranged from 0 to 96.9 % (mean = 8.1 %). The results indicated that fog water deposition contributed significantly to acid deposition in some mountainous areas in the Kinki Region of Japan.

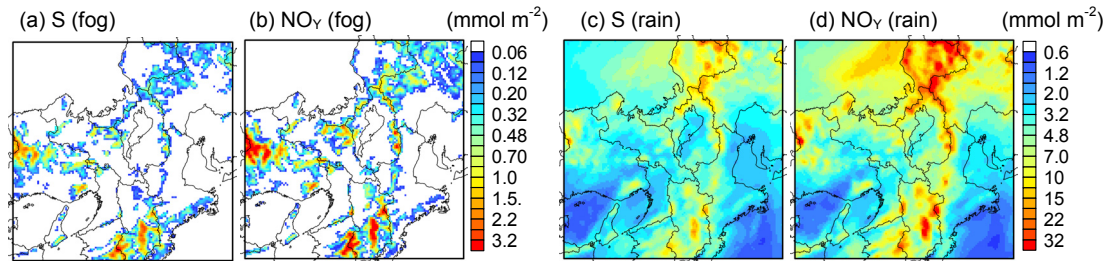


Figure 8. Spatial distributions of model-predicted (a) S and (b) NO_Y depositions through fog, and (c) S and (d) NO_Y depositions through rain in D4 in March 2005.

CONCLUSION

The present study developed FDM to predict fog water deposition in forest areas. The values of V_{Dep} calculated by FDM considerably varied with u and parameters on forest. In Comparison of FDM with the field measurement data, while the total fog water deposition predicted by FDM agreed with the measurement, large discrepancies often occurred between FDM and the measurement. Additional comparisons of FDM with other measurements may help to reveal the cause of the discrepancies. Moreover, this study estimated fog water deposition and corresponding S and NO_Y depositions with FDM and the MM5/CMAQ modelling system in the Kinki Region of Japan in March 2005. The results indicate that fog water deposition can contribute significantly to acid deposition in some mountainous areas in the region. The contribution of fog to acid deposition may considerably vary with seasonal variations in meteorology, air quality and vegetation structure. Therefore, long-term prediction (1year ~) is required for further discussion.

REFERENCES

- Aikawa, M., Hiraki, T. and Tamaki, M., 2006: Comparative field study on precipitation, throughfall, stemflow, fog water, and atmospheric aerosol and gases at urban and rural sites in Japan. *Sci. Tot. Environ.*, **366** (1), 275-285.
- Baumgardner, R.E., Kronmiller, K.G., Anderson, J.B., Bowser, J.J. and Edgerton, E.S., 2003: Estimates of cloud water deposition at mountain acid deposition program sites in the Appalachian Mountains. *Atmos. Environ.*, **33** (30), 5105-5114.
- Burkard, R., Butzberger, P. and Eugster, W., 2003: Vertical fogwater flux measurements above an elevated forest canopy at the Lägeren research site, Switzerland. *Atmos. Environ.*, **37** (21), 2979-2990.
- Byun, D.W. and Ching, J.K.S., 1999: Science Algorithms of the EPA Models-3 Community Multi-scale Air Quality (CMAQ) Modeling System. NERL, Research Triangle Park, NC.
- Dawson, T.E., 1998: Fog in the California redwood forest: Ecosystem inputs and use by plants. *Oecol.*, **117** (4), 476-485.
- Grell, G.A., Dudhia, J. and Stauffer, D.R., 1994: A description of the fifth-generation Penn State/NCAR mesoscale model (MM5). NCAR Technical Note NCAR/TN-398+STR, 117 pp.
- Katata, G., Nagai, H., Wrzesinsky, T., Klemm, O., Eugster, W. and Burkard, R., 2008: Development of a land surface model including cloud water deposition on vegetation. *J Appl. Meteorol. Climatol.*, **47** (8), 2129-2146.
- Klemm, O., Wrzesinsky, T. and Scheer, C., 2005: Fog water flux at a canopy top: Direct measurement versus one-dimensional model. *Atmos. Environ.*, **39**, 5375-5386.
- Kobayashi, T., Nakagawa, Y., Tamaki, M., Hiraki, T. and Aikawa, M., 2001: Cloud water deposition to forest canopies of *Cryptomeria japonica* at Mt. Rokko, Kobe, Japan. *Water Air Soil Pollut.*, **130** (1-4 II), 601-606.
- Kondo, J. and Akashi, S., 1976: Numerical studies on the two-dimensional flow in horizontally homogeneous canopy layers. *Boundary-Layer Meteorol.*, **10** (3), 255-272.
- Lovett, G.M., 1984: Rates and mechanisms of cloud water deposition to a subalpine balsam fir forest. *Atmos. Environ.*, **18**, 361-371.
- Miller, E.K., Panek, J.A., Friedland, A.J., Kadlecsek, J. and Mohnen, V.A., 1993: Atmospheric deposition to a high-elevation forest at Whiteface Mountain, New York, USA. *Tellus*, **45B**: 209-227.
- Nagai, H., 2002: Validation and sensitivity analysis of a new atmosphere-soil-vegetation model. *J Appl. Meteorol.*, **41** (2), 160-176.
- Neal, C., Reynolds, B., Neal, M., Hill, L., Wickham, H. and Pugh, B., 2003: Nitrogen in rainfall, cloud water, throughfall, stemflow, stream water and groundwater for the Plynlimon catchments of mid-Wales. *Sci. Tot. Environ.*, **314-316**, 121-151.
- Shimadera, H., Kondo, A., Kaga, A., Shrestha, K.L. and Inoue, Y., 2009: Contribution of transboundary air pollution to ionic concentrations in fog in the Kinki Region of Japan. *Atmos. Environ.*, **43** (37), 5894-5907.
- Vong, R.J., Sigmon, J.T. and Mueller, S.F., 1991: Cloud water deposition to appalachian forests. *Environ. Sci. Technol.* **25** (6), 1014-1021.
- Yamada, T., 1982: A Numerical Model Study of Turbulent Airflow In and Above a Forest Canopy. *J. Meteorol. Soc. Japan*, **60**, 439-454.